SEECCM 2017

4th South-East European Conference on Computational Mechanics

03-04 July, Kragujevac, Serbia

Organizers

Serbian Society for Computational Mechanics

Bioengineering Research and Development Center BioIRC

European Community on Computational Methods in Applied Sciences ECCOMAS

Department of Technical Sciences Serbian Academy of Sciences and Arts

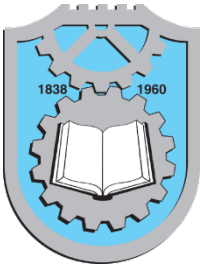

Faculty of Engineering University of Kragujevac

Ministry of Education, Science and Technological Development of Republic of Serbia

ISBN: 978-86-921243-0-3

Contents

Session M.2 - 12:30-13:10
Mechanics
Chair: Milica Nikolić

M.2.1 - *Simulation of Fracture and Delamination in Layered Shells Due to Blade Cutting*
Federica Confalonieri, Umberto Perego

M.2.2 - *Theory of Ambient Vibration Energy Harvester with Piezoelement*
Livija Cvetićanin, D. Cvetićanin

M.2.3 - *Lifetime Prediction of Cardiovascular Stent Based on Fatigue to Fracture Approach*

Gordana Jovičić, Arso Vukicević, Dalibor Nikolić, Nenad Filipović

M.2.4 - *Analysis of Loads and Deformation of Valve Plate in Contact with Cylinder Block at Axial Piston Pump for Water Hydraulics*
Nenad Todić, Snežana Vulović, Miroslav Živković, Slobodan Savić, Vesna Ranković

Session M.3 – 13:10-14:00
Data Mining
Chair: Bojana Anđelković Ćirković

M.3.1 - *Automatic Main Pulmonary Artery Identification on Chest CT using Supervised Machine Learning*
Daniel A. Moses, Laughlin Dawes, Claude Sammut, Tatjana Zrimec

M.3.2 - *Framework for creation of customized shape of the shoe insole*
Suzana Petrović Savić, Zoran Jovanović, Goran Devedžić

M.3.3 - *Multiscale Microstructural Optimization of Carbon Nanotube/Polymer Structures using Genetic Algorithms*
Maria Tavlaki, Odysseas Kokkinos, Vissarion Papadopoulos, Manolis Papadrakakis

M.3.4 - *Analysis of Layer Recurrent Network to Estimate Nondimensional Velocity of the Dissociated Gas*
Vesna Ranković, Slobodan Savić, Nenad S. Todić

M.3.5 - *Prediction of Second Primary Tumors in Patients with Oral Squamous Cell Carcinoma*
Bojana Anđelković Ćirković, Daniela Elena Costea, Nenad Filipović

14:00 - 15:00	Buffet Lunch

15:00 - 15:30	Keynote speaker: **"A multiphase porous media model for transport oncophysics"** **Prof. Bernhard Schrefler** *University of Padova, Italy*

15:30 - 16:00	Keynote speaker: **"Computational models and Data – a Possible Fusion"** **Prof. Hermann Matthies** *Braunschweig University of Technology, Germany*

16:00 - 16:30	Coffee Break

Book of Abstracts

The current work proposes a novel three-level multiscale optimization technique to optimize the orientation and dispersion of nanotubes in several benchmark carbon nanotube-polymer structures: a) At the atomic level, a nanotube was modeled as a space-frame structure using mMSM. b) At the microscopic level, a Representative Volume Element consisting of a straight nanotube embedded in polymer was analyzed using a first-order homogenization technique. c) Finally, at the highest level, a macroscopic structure was analyzed concurrently with the previous level using a nested solution scheme. One RVE corresponding to a nanotube orientation and diameter was assigned to every element of the macroscopic structure. Using the NSGA-II multi-objective optimization algorithm, a set of nanotube angles and diameters was calculated so that the energy for each macroscopic structure was minimized, under the constraint that the mean nanotube volume fraction over the structure has to remain constant.

M.3.4 - *Analysis of Layer Recurrent Network to Estimate Nondimensional Velocity of the Dissociated Gas* - Vesna Ranković, Slobodan Savić, Nenad S. Todić

In this paper a layer recurrent neural network has been used to predict the nondimensional velocity of the gas that flows along a porous wall. Equations were analyzed using finite difference method and data has been obtained from a CFD-based computer code. The activation functions of the hidden nodes are hyperbolic tangent sigmoid transfer function. Results of simulations show that the application of the layer digital recurrent neural network to predict the velocity of the gas gives satisfactory results. The performance of the network model has been assessed through the correlation coefficient.

M.3.5 - *Prediction of Second Primary Tumors in Patients with Oral Squamous Cell Carcinoma* - Bojana Anđelković Ćirković, Daniela Elena Costea, Nenad Filipovic

Oral squamous cell carcinoma (OSCC) is the most common malignant head tumor. Patients with OSCC are at increased risk for the development of a second primary malignancy, which is defined as a second malignancy that presents either simultaneously or after the diagnosis of an index tumor. This study aimed to develop data mining prediction model for the occurrence of second primary tumors (SPT) for OSCC patients. Methodology approach based on genetic algorithm (GA) and artificial neural network (ANN) was used to perform automatic feature selection as well as design of the classifier structure and tuning of classifiers' parameters. The algorithms were successfully applied to the novel data set of 95 patients with OSCC. Our results suggest that we developed the optimized ANN model for prediction of second primary tumors in OSCC patients with high accuracy. The model could help clinicians to tailor the treatment plan and adopt follow - up strategy to efficiently manage the OSCC disease.

Session M.4 - 18:00-19:30
Finite Element Modelling

Chair: Aleksandra Vulović

M.4.1 - *Finite Element Modelling of Rotary Transfer Machines* - Alberto Martini, Marco Troncossi, Nicolò Vincenzi

Vibration monitoring and control are central topics for machine tools, since high vibration levels reduce the quality of machined surfaces and shorten the tool life. In order to predict potential vibration issues since the early design stage, it is necessary to implement ad hoc numerical models for modal analysis. This requires significant efforts and possible conflicts with tight production scheduling of companies. This work focuses on a specific family of rotary transfer machines for the manufacturing of parts related to lock&keys industry. It investigates the possibility to achieve an acceptable estimation of the elastodynamic behavior of the machine tools through limited modifications of the Finite Element (FE) models used for structural analysis, which are generally available in the early phases of the design process. The structural FE model of a new machine tool is implemented and validated through experimental tests performed on a prototype. Then, the elastodynamic FE model is derived and simulated, and the numerical results are presented.

M.4.2 - *Investigating Low Velocity Impact on Biocomposites by MAT_54 Shell Modeling* - Felipe Vannucchi de Camargo, Ana Pavlović

Biocomposites have risen as an alternative for supplying the sustainability concern in the composites field, and as in any emergent structural technology, there is a need to quantify the characteristics of such materials by experimental testing and numerical simulations. Among the important tests required to provide a wide comprehension of the material properties, the evaluation of low-velocity impact resistance is essential for allowing its application on structural components. Given the explicit shell material MAT_54 of LS-DYNA used in simulations of such kind to represent the slave part, the present work thoroughly studies the influence of some of its most important immeasurable parameters that demand calibration to understand their influence on a low-velocity impact condition.

M.4.3 - *Finite Element Modeling in Palletized Products Under Transportation* - João Pedro Teixeira Peixoto de Queiroz, Antonio Carlos de Figueiredo Silveira, Felipe Vannucchi de Camargo

Analysis of Layer Recurrent Network to Estimate Nondimensional Velocity of the Dissociated Gas

Vesna Ranković[1], Slobodan Savić[1*], Nenad S. Todić[1]

[1] University of Kragujevac, Faculty of Engineering, 6 Sestre Janjić Street, Kragujevac, Serbia
e-mail: vesnar@kg.ac.rs, ssavic@kg.ac.rs, ntodic@gmail.com

**corresponding author*

Abstract

In this paper a layer recurrent neural network has been used to predict the nondimensional velocity of the gas that flows along a porous wall. Equations were analyzed using finite difference method and data has been obtained from a CFD-based computer code. The activation functions of the hidden nodes are hyperbolic tangent sigmoid transfer function. Results of simulations show that the application of the layer digital recurrent neural network to predict the velocity of the gas gives satisfactory results. The performance of the network model has been assessed through the correlation coefficient.

Keywords: Recurrent Network, Dissociated Gas, Prediction, Velocity

1. Introduction

A series of problems in engineering can be modeled with a set of differential equations. Many methods have been proposed in the relevant literature to solve differential equations such as the finite element method, finite difference method, finite volume method and the boundary element method, Glowinski and Neittaanmaki (2008). Beside these basic methods, some researchers have utilized the approximation properties of multilayer perceptrons (He, Reif and Unbehauen, 2000; Vaziri et al., 2007), radial basis function network (Chen, Kong and Leng, 2011; Mai-Duy, 2005), adaptive network-based fuzzy inference system (Yazdi and Pourreza, 2010) to solve differential equations reducing cost of studies and saving computational time.
The soft computing methodologies have been applied to predict results in computational and experimental heat transfer and fluid dynamics studies (Vaziri et al., 2007; Guanghui et al., 2003; Mahmoud and Ben-Nakhi, 2007).

In this paper, the feasibility of using Layer Digital Recurrent Neural Network (LDRNN) to predict new cases of the nondimensional velocity of the dissociated gas has been studied. The recurrent neural network trained on a database generated by a computational fluid dynamics analysis has been used to save effort and computation time in numerical studies. In Section 2, the governing equations for the ideally air flow has been presented. A database has been generated by using finite difference method. Section 3 and Section 4 describe digital recurrent neural network and model results. Finally, in Section 5 concluding remarks have been given.

2. Data generation with CFD code

The governing equations for the ideal air flow along a porous wall of the body of revolution within the fluid in the conditions of equilibrium dissociation can be given as follows (Schlichting, 1974):

$$\frac{\partial}{\partial x}(\rho u r)+\frac{\partial}{\partial y}(\rho v r)=0 \tag{1}$$

$$\rho u\,\frac{\partial u}{\partial x}+\rho v\,\frac{\partial u}{\partial y}=\rho_e u_e\,\frac{du_e}{dx}+\frac{\partial}{\partial y}\left(\mu\,\frac{\partial u}{\partial y}\right) \tag{2}$$

$$\rho u\,\frac{\partial h}{\partial x}+\rho v\,\frac{\partial h}{\partial y}=-u\,\rho_e u_e\,\frac{du_e}{dx}+\mu\left(\frac{\partial u}{\partial y}\right)^2+\frac{\partial}{\partial y}\left[\frac{\mu}{\mathrm{Pr}}(1+l)\frac{\partial h}{\partial y}\right] \tag{3}$$

$$\begin{aligned} &u=0, \quad v=v_w(x), \quad h=h_w \quad \text{for} \quad y=0\\ &u\to u_e(x), \quad\quad\quad h\to h_e(x) \quad \text{for} \quad y\to\infty. \end{aligned} \tag{4}$$

The equation (1) is a continuity equation of axisymmetrical compressible fluid flow on bodies of revolution, the eq. (2) one is dynamic, and the eq. (3) one is energy equation. The function $l(p, h)$ for the equilibrium two-componential mixture depends on Lewis number Le and on the enthalpy of the atomic h_A and molecular h_M components of the equilibrium dissociated gas (air). This function is determined with the expression (Obrovic, Nikodijevic and Savic, 2009).

$$l(p,\,h)=(\mathrm{Le}-1)(h_A-h_M)\left(\frac{\partial C_A}{\partial h}\right)_p. \tag{5}$$

Here the following notation is used: $u(x, y)$ - the longitudinal projection of the velocity in the boundary layer, $v(x,\ y)$ - transversal projection, ρ - density of the ideally dissociated gas, μ - dynamic viscosity, h - enthalpy. Here, x and y are longitudinal and transversal coordinates, respectively. Prandtl and Lewis numbers are defined with the expressions: $\mathrm{Pr}=\mu c_p/\lambda$, $\mathrm{Le}=\rho c_p D/\lambda$ in which λ - stands for the thermal conductivity coefficient, c_p - specific heat of the dissociated gas at constant pressure and D - atomic component diffusion coefficient. The radius of the cross-section of the body of revolution, which is normal to the axis of revolution, is denoted with $r(x)$. The contour of the body, which figures in the continuity equation is given by the function $r(x)$. The subscript $''e''$ denotes the physical quantities at the outer edge of the boundary layer, and the subscript $''w''$ stands for the quantities at the wall of the body within the fluid. Here, $v_w(x)$ denotes the given velocity of the gas that flows through the solid porous wall ($v_w>0$ or $v_w<0$).

When the governing equation system is transformed (1)-(4) and when the change (Saljnikov and Dallmann, 1989)

$$\frac{u}{u_e}=\frac{\partial \Phi}{\partial \eta}=\varphi=\varphi(\eta,\,\kappa,\,f,\,\Lambda) \tag{6}$$

that decreases the order of the differential equations is performed (Obrovic, Nikodijevic and Savic, 2009), a generalized equation system with four independent variables, η, κ, f and Λ, is obtained

$$\frac{\partial}{\partial\eta}\left(Q\frac{\partial\varphi}{\partial\eta}\right)+\frac{aB^2+(2-b)f}{2B^2}\Phi\frac{\partial\varphi}{\partial\eta}+\frac{f}{B^2}\left(\frac{\bar{h}}{1-\kappa}-\varphi^2\right)+\frac{\Lambda}{B}\frac{\partial\varphi}{\partial\eta}=$$
$$=\frac{F_{ot}f}{B^2}\left(\varphi\frac{\partial\varphi}{\partial f}-\frac{\partial\Phi}{\partial f}\frac{\partial\varphi}{\partial\eta}\right) \tag{7}$$

$$\frac{\partial}{\partial\eta}\left(\frac{Q}{\mathrm{Pr}}\frac{\partial\bar{h}}{\partial\eta}\right)+\frac{aB^2+(2-b)f}{2B^2}\Phi\frac{\partial\bar{h}}{\partial\eta}-\frac{2\kappa f}{B^2}\varphi\left(\frac{\bar{h}}{1-\kappa}-\varphi^2\right)+2\kappa Q\left(\frac{\partial\varphi}{\partial\eta}\right)^2+$$
$$+\frac{\Lambda}{B}\frac{\partial\bar{h}}{\partial\eta}=\frac{F_{ot}f}{B^2}\left(\varphi\frac{\partial\bar{h}}{\partial f}-\frac{\partial\Phi}{\partial f}\frac{\partial\bar{h}}{\partial\eta}\right) \tag{8}$$

$$\begin{aligned}&\Phi=0,\ \varphi=0,\quad \bar{h}=\bar{h}_w=const.\quad \text{for}\ \ \eta=0,\\ &\varphi\to1,\qquad\quad \bar{h}\to\bar{h}_e=1-\kappa\quad \text{for}\ \ \eta\to\infty.\end{aligned} \tag{9}$$

The usual notation is used. Thus, u/u_e - nondimensional velocity, Φ - nondimensional stream function, η - nondimensional transversal coordinate, κ - compressibility parameter, f - form parameter, Λ - porosity parameter, $\bar{h}$ - nondimensional enthalpy, Q - nondimensional function, B - characteristics of the boundary layer, F_{ot} - characteristic boundary layer function, and a, b - constants. The equations are solved for the following values of the parameters and coefficients: $\mathrm{Pr}=0.712$; $a=0.4408$; $b=5.7140$ (Saljnikov and Dallmann, 1989).

Numerical solutions of the obtained generalized partial differential equations are first obtained for each cross-section of the boundary layer, by the finite difference method. Here, the whole area of the boundary layer is changed with the planar integration grid. The numerical solution is applied for training and testing the LDRNN. Data has been generated for $\Lambda=[-0.1\ \ 0.1]$, $f=[-0.16\ \ 0.16]$ and $\eta=[0\ \ 20]$.

3. Digital recurrent neural network

In this paper two layered digital recurrent network (Fig. 1) with sigmoid neurons in the hidden layer and linear neuron in the output layer has been used.

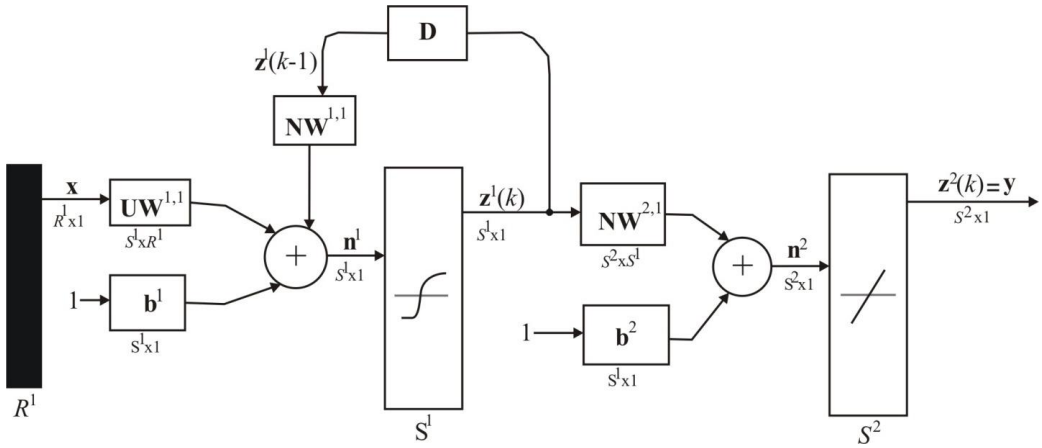

Fig. 1. Digital recurrent neural network.

The layered digital recurrent network differs from two-layer percrptron network in that the first layer has a recurrent connection. The delay in this connection stores values from the previous time step, which can be used in the current time step. LDRNN network can approximate any function with a finite number of discontinuities to any degree of accuracy.

In Fig. 1, elements of layer *i*, such as its bias, net input, and output have a superscript *i* to denote that they are associated with the *i*-th layer; $\mathbf{x}$ is an *R* length input vector; S^i, $i = 1,2$ is the number of neurons of the *i*-th layer; the weight matrix connected to the input vector $\mathbf{x}$ is labeled as an input weight matrix ($\mathbf{UW}^{1,1}$); $\mathbf{NW}^{1,1}$ and $\mathbf{NW}^{2,1}$ are matrices of weights of the connections between the recurrent and the hidden units, and between the hidden and the output units, respectively; $\mathbf{b}^1$ and $\mathbf{b}^2$ are vectors of biases of hidden neurons and output units, $\mathbf{z}^1$ and $\mathbf{z}^2$ are vectors of outputs of hidden neurons and output units.

The output $\mathbf{z}^1(k)$ at recurrent tansig layer can be calculated as:

$$\mathbf{z}^1(k) = \mathbf{tansig}\left(\mathbf{n}^1\right) \tag{1}$$

or:

$$\mathbf{z}^1(k) = \frac{2}{1+e^{-2\mathbf{n}^1}} \tag{2}$$

where:

$$\mathbf{n}^1 = \mathbf{x}\cdot\mathbf{UW}^{1,1} + \mathbf{NW}^{1,1}\cdot\mathbf{z}^1(k-1) + \mathbf{b}^1 \tag{3}$$

The output of the network is determined as:

$$\mathbf{z}^2(k) = \mathbf{purelin}\left(\mathbf{n}^2\right) \tag{4}$$

or:

$$\mathbf{z}^2(k) = k\cdot\left(\mathbf{n}^2\right) \tag{5}$$

where:

$$\mathbf{n}^2 = \mathbf{NW}^{2,1}\cdot\mathbf{z}^1(k) + \mathbf{b}^2 \tag{6}$$

The output of the network is a function not only of the weights, biases, and network input, but also of the outputs of hidden neurons at previous points in time. Hagan, Jesus and Schultz (1999) developed the versions of the backpropagation training are used to adapt weights and biases of the LDRN network.

4. Simulation results

Data were generated using the finite differences method and has been divided into training, validation and test subsets. The Pearson correlation coefficient is used to define degree of correlation between the values obtained from the CFD code and the predicted values by the recurrent neural network. Several recurrent networks have been generated and tested.

In this paper, the trial and error method has been applied to determine the number of neuron in hidden layer. The optimal number of neurons in the hidden layer has been determined based on a large number of repeated experiments with different number of hidden layer

neurons. The number of hidden neurons has been considered between 3 and 15. The optimal network size was the one which resulted in a maximum correlation coefficient for the training and test set. The optimal number of hidden neurons is 10. The performance parameters of the recurrent neural network models for computation of the u/u_e are given in Table 2.

Recurrent neural network-structure 3-10-1	***set***	***r***
	Training	0.9843
	Validation	0.9811
	Test	0.9799
	Training + Validation + Test	0.982

Table 2. Performance parameters of the recurrent neural network models for computation of the u/u_e.

The input weight matrix, the matrices of weights of the connections between the recurrent and the hidden units, and between the hidden and the output units, vectors of biases of hidden neurons and output units of the trained recurrent neural network are:

$\mathbf{UW}^{1,1}$ =[1.18 –0.699 0.576;
1.18 0.61 2.52;
–0.658 0.38 –0.274;
0.12 –0.047 3.825;
0.334 –0.745 1.9;
–1.256 0.84 –1.997;
1.055 –0.336 –0.035;
–0.726 –0.264 1.473;
0.736 0.118 4.706;
–1.644 0.315 –1.766]

$\mathbf{NW}^{1,1}$ =[0.346 –0.103 – 0.376 0.422 0.573 –0.249 –0.713 –0.568 –0.083 –0.661;
–0.588 –0.149 0.225 –0.308 –0.309 0.416 –0.561 0.37 –0.523 0.58;
–0.36 0.428 0.25 0.01 0.506 0.137 0.0496 –0.304 –0.437 –0.798;
–0.693 0.45 –0.515 0.304 –0.391 0.076 0.426 0.044 0.631 0.419;
–0.536 –0.417 –0.507 0.52 0.571 0.556 0.577 –0.445 –0.463 0.422;
0.509 –0.0161 –0.0026 0.722 –0.236 –0.337 –0.582 0.16 0.512 0.58;
0.373 –0.104 0.88 0.09 –0.581 0.49 0.132 –0.454 0.073 –0.796;
–0.341 0.273 –0.297 –0.673 –0.464 0.473 –0.057 0.287 0.924 –0.187;
0.678 0.315 0.128 –0.528 0.175 –0.1799 –0.735 0.285 –0.635 –0.361;
–0.729 0.399 –0.433 –0.38 –0.0418 0.106 –0.255 0.389 –0.09 0.47]

$\mathbf{NW}^{2,1}$ =[0.262 0.099 –0.109 –0.928 –0.348 –0.489 –0.2699 1.576 1.835 0.274]

$\mathbf{b}^1$ =[–0.572; 0.054; 1.855; 2.643; 0.0657; –0.852; –0.131; 2.366; 3.817; –0.896]

$\mathbf{b}^2$ =[–1.382]

Fig. 2 and Fig.3 are diagrams of the nondimensional velocity u/u_e for three cross sections of the boundary layer.

5. Conclusions

The proposed learning system, constructed as an intelligent computing technique, relies on the function approximation capabilities of layer digital recurrent neural networks. By comparing the proposed method results with finite difference method the accuracy of the method has been proven.

The recurrent neural networks are excellent function approximators and allows us to obtain a fast and accurate solution of partial differential equations. Recurrent networks have advantage over a feedforward network in prediction and analysis of complex systems.

Finally, it should be pointed out that the number of neuron in the hidden layer is very important for forecasting the ability of recurrent network and computational cost.

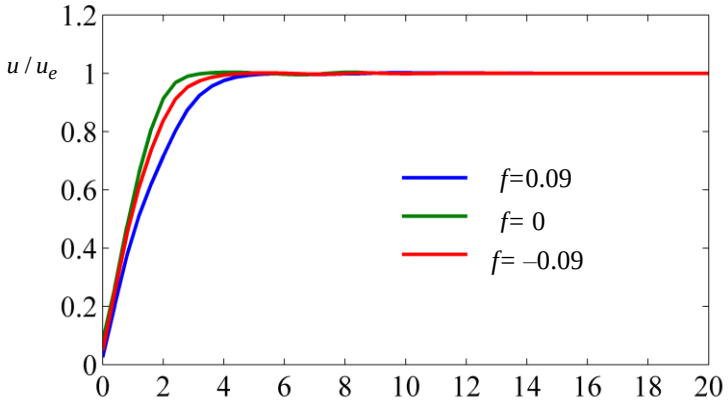

Fig. 2. Diagram of the nondimensional velocity ($\Lambda = 0.07$)

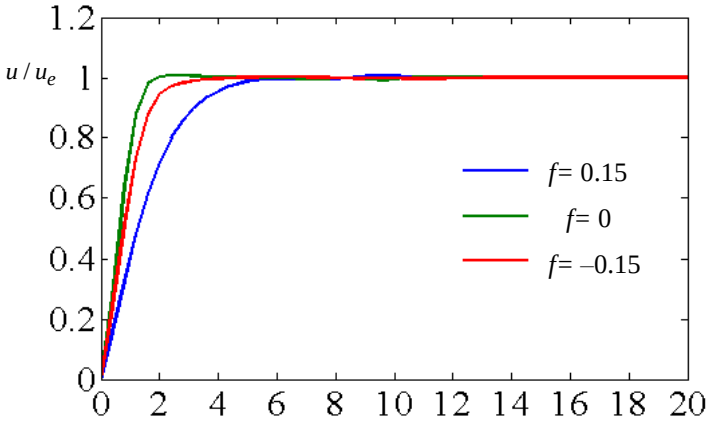

Fig. 3. Diagram of the nondimensional velocity ($\Lambda = 0.1$)

Acknowledgements The research was supported by the Ministry of Education, Science and Technological Development of the Republic of Serbia, grants III41007 and OI 174014.

References

Chen H, Kong L, Leng W (2011). Numerical solution of PDEs via integrated radial basis function networks with adaptive training algorithm, *Applied Soft Computing*, 11, 855-860.

Glowinski R, Neittaanmaki P (2008). *Partial Differential Equations: Modeling and Numerical Simulation*, Springer.

Guanghui S, Morita K, Fukuda K, Pidduck M, Dounan J, Miettinen J (2003) . Analysis of the critical heat flux in round vertical tubes under low pressure and flow oscillation conditions. Applications of artificial neural network, *Nuclear Engineering and Design,* 220, 17-35.

Hagan M, Jesus O D, Schultz R (1999). Training Recurrent Networks for Filtering and Control, *Chapter 11 of Recurrent Neural Networks: Design and Applications*, L.R. Medsker and L.C. Jain, Eds., CARC Press, pp. 325-354.

He S, Reif K, Unbehauen R (2000). Multilayer neural networks for solving a class of partial differential equations, *Neural Networks*, 13, 385-396.

Mahmoud M A, Ben-Nakhi A E (2007). Neural networks analysis of free laminar convection heat transfer in a partitioned enclosure, *Communications in Nonlinear Science and Numerical Simulation,* 12, 1265–1276.

Mai-Duy N (2005). Solving high order ordinary differential equations with radial basis function networks, *International Journal for Numerical Methods in Engineering*, 62, 824-852.

Obrovic B, Nikodijevic D, Savic S (2009). Boundary layer of dissociated gas on bodies of revolution of a porous contour, *Strojniski vestnik - Journal of Mechanical Engineering*, 55(4), 244-253.

Saljnikov V N, Dallmann U (1989). *Verallgemeinerte Ähnlichkeitslösungen für dreidimensionale, laminare, stationäre, kompressible Grenzschichtströmungen an schiebenden profilierten Zylindern.* Institut für Theoretische Strömungsmechanik DLR-FB 89-34, Göttingen.

Schlichting H (1974). *Grenzschicht-theorie.* Verlag G. Braun, Karlsruhe.

Shirvany Y, Hayati M, Moradian R (2009). Multilayer perceptron neural network with novel unsupervised training method for the solution of partial differential equations, *Applied Soft Computing*, 9, 20-29.

Yazdi H S, Pourreza R (2010). Unsupervised adaptive neural-fuzzy inference system for solving differential equations, *Applied Soft Computing*, 10(1), 267-275.

Vaziri N, Hojabri A, Erfani A, Monsefi M, Nilforooshan B (2007). Critical heat flux prediction by using radial basis function and multilayer perceptron neural networks: a comparison study, *Nuclear Engineering and Design,* 237, 377-385.